Heliyon 10 (2024) e36032

Contents lists available at ScienceDirect

Heliyon

journal homepage: www.cell.com/heliyon

Research article

Belamcanda chinensis extract inhibits non-small cell lung cancer proliferation and induces apoptosis via inhibiting the MAPK (Ras/Raf) and Akt pathways

Chong Ma [a,b,1], Jingyi Yin [a,b,1], Xiao Feng [a,b,1], Xin Wang [a,b], Xiaodie Cao [a,b], Chen Zhang [a,b], Rongjie Cui [a,b], Jingru Wei [a,b], Xu He [b,c], Yan Li [b,c,**], Li Chen [a,b,*]

[a] *Department of Pathophysiology, School of Basic Medicine, Kunming University of Science and Technology, Kunming, China*
[b] *The First People's Hospital of Yunnan Province, The Affiliated Hospital of Kunming University of Science and Technology, Kunming, China*
[c] *Department of Geriatrics, The First People's Hospital of Yunnan Province, Kunming, China*

ARTICLE INFO

Keywords:
The non-small cell lung cancer
Belamcanda chinensis extract
Proliferation
Apoptosis
Ras
Raf
MAPK
Akt

ABSTRACT

Non-small cell lung cancer (NSCLC) is associated with high mortality and morbidity rates. Despite major progress of treatment of NSCLC over the past few decades, the prognosis of advanced NSCLC is poor, with 5-year survival rates ranging from 2 % to 13 %. *Belamcanda chinensis* is a traditional Chinese medicine used to promote blood circulation, reduce swelling, heal ulcers, disperse lumps and tumors, and resolve blood stasis. In the present study, the anti-proliferative and pro-apoptotic effects and potential mechanisms of action of *Belamcanda chinensis* extract (BCE) in SPC-A1 and NCI–H460 NSCLC cells were investigated using MTS, flow cytometry, and western blotting. Also, xenograft model *in vivo* was established to investigate the anti-NSCLC effects of BCE. The compounds in BCE were quantified using gas chromatography-mass spectrometry (GC-MS). Twenty compounds were found in BCE, and BCE induced cell cycle arrest significantly inhibited the proliferation of NSCLC. Furthermore, BCE was found to induce Cyto C release and the activation of Caspase-3, -8, -9, PARP, ultimately inducing apoptosis in NSCLC cells through both exogenous and endogenous apoptotic pathways (the mitochondrial pathway). BCE also blocked the MAPK (Ras/Raf) and Akt signaling pathways, significantly downregulating the expression of Ras, Raf, Erk1/2, p-Erk1/2, Akt, and p-Akt proteins. Furthermore, BCE significantly inhibited the growth of NSCLC cells SPC-A1 in nude mice and downregulated Ras, Raf, Akt, and p-Akt expression *in vivo*. The antitumor effects of BCE suggest its potential clinical application in patients with NSCLC, especially in those bearing Ras or Raf mutations.

1. Introduction

Lung cancer is characterized by high morbidity, poor prognosis, and high fatality rate. About 1.6 million people die each year from this malignant tumor [1–3]. According to 2020 statistics, lung cancer accounts for 11.4 % of all cancer cases [4]. NSCLC is the predominant pathological type, accounting for 80%–85 % of all lung cancers [5]. Owing to the hidden early symptoms of the disease, most

* Corresponding author. School of Basic Medicine, Kunming University of Science and Technology, 650500, China.
** Corresponding author. Department of Geriatrics, The First People's Hospital of Yunnan Province, 650100, China.
E-mail addresses: liyanken@126.com (Y. Li), atlanis@qq.com (L. Chen).
[1] Contributed equally.

https://doi.org/10.1016/j.heliyon.2024.e36032
Received 22 April 2024; Received in revised form 30 July 2024; Accepted 8 August 2024
Available online 9 August 2024

newly diagnosed patients develop advanced disease. In addition, most diagnosed patients are old and have poor tolerance to conventional therapies, such as surgery, radiotherapy, and chemotherapy, which limits the use of conventional treatments [6–8]. Although small-molecule targeted therapies with high specificity and few toxic side effects have emerged in the past two decades, drug resistance has inevitably emerged in many patients, eventually leading to treatment failure [9–11]. From the molecular mechanism of lung cancer onset, it is known that the mitogen-activated protein kinase (MAPK/Ras-Raf-Mek-Erk1/2) pathway is the main pathway for lung cancer development [12,13]. Regardless of the presence of epidermal growth factor receptor (EGFR) mutations [14], Ras mutations [15], or echinoderm microtubule-associated protein-like 4-anaplastic lymphoma kinase (EML4-ALK) fusion gene [16], Ras-Raf signaling is transmitted and eventually activates Erk1/2, promoting the malignant proliferation of lung cancer cells. The discovery of mutated or fused genes that drive lung cancer cell proliferation and tumor growth has led to the development of highly effective targeted drugs. Some target-directed therapies involving drugs such as EGFR tyrosine kinase inhibitors (erlotinib, gefitinib, osimertinib, and afatinib) and ALK inhibitors (crizotinib, certinib, and alectinib) have already been approved for clinical use. Although targeted drugs are beneficial for the treatment of lung cancer, most patients inevitably develop resistance to targeted drugs, leading to treatment failure [17,18]. The mechanism of resistance to targeted drugs is complex and includes the re-mutation of the oncogenes mentioned above, activation of bypass pathways, and histological changes. For example, the EGFR-T790M mutation is resistant to erlotinib and gefitinib [18–20], while the L1196M and C1156Y mutations in ALK are resistant to crizotinib [20,21]. Epithelial-mesenchymal transition (EMT) is one of the mechanisms leading to TKI resistance [21,22]. As KRAS mutations cannot be used as drug targets, few targeted drugs are available for patients with KRAS mutations [22,23]. In addition, up to 40 % of lung adenocarcinomas do not contain the oncogenes that drive cancer development [24,25].

Traditional Chinese medicines (TCM) have distinct mechanisms of action. TCM could potentially sensitize tumors that are normally resistant to conventional chemotherapy while diminishing their side effects [26–28]. Chinese medicine believes that the stagnation of heat is an important factor affecting the occurrence and development of tumors; therefore, clearing heat and detoxifying it are important concepts in the treatment of tumors in TCM [29,30]. *Belamcanda chinensis* is the dried root of *Belamcanda chinensis* (L.) DC, and it is not a protected or endangered species. It is collected in early spring or autumn after 2–3 years of cultivation [31]. *Belamcanda chinensis* is used in antipyretic agents, analgesics, antiphlogistics, expectorants, and antidotes [32]. In recent decades, the pharmacological activities of *Belamcandae chinensis* and its compounds have been reported, showing significant effects on several tumor types, including triple-negative breast cancer [33], human osteosarcoma cells [34], prostate cancer [35], and malignant testicular germ cell carcinoma [36]. However, it is interesting to note that extracts of *Belamcanda chinensis* have been reported to exhibit stronger antitumor activity than monomer compounds [37]. In the present study, we analyzed the chemical composition of *Belamcanda chinensis* extract (BCE) and evaluated its antitumor effects in two types of NSCLC cell lines, SPC-A1 and NCI–H460, to explore the possible antitumor mechanism in NSCLC and provide further theoretical support for its future clinical application.

2. Materials and methods

2.1. Chemical reagents and antibodies

phenazine methosulfate (PMS) and 3-(4,5-dimethylthiazol-2-yl)-5-(3-carboxymethoxyphenyl)-2-(4-sulfophenyl)-2H-tetra-zolium (MTS) were obtained from Promega (Beijing, China). MG132 (a proteasome inhibitor), mouse monoclonal antibody against β-actin, Dimethyl sulfoxide (DMSO), Z-VAD-FMK (a well-known pan Caspase inhibitor), propidium iodide (PI) and Annexin V-FITC Apoptosis Detection Kit were brought from Sigma Aldrich (Shanghai, China). Antibodies (Cell Signaling Technology, Shanghai, China) against the following proteins were used: Ras, Raf, Caspase-3, Caspase-8, Caspase-9, poly (adenosine diphosphate [ADP]-ribose) polymerase (PARP), Erk1/2, cytochrome *c* (Cyto C), phospho-Erk1/2 (p-Erk1/2), protein kinase B (Akt), phospho-Akt (p-Akt). The TRIzol reagent was obtained from Invitrogen (Thermo Fisher Scientific, USA).Secondary antibodies were purchased from Santa Cruz Biotechnology (Shanghai, China). Dulbecco's modified Eagle's medium (DMEM), Roswell Park Memorial Institute 1640 medium (RPMI 1640) and fetal bovine serum (FBS) were purchased from Gibco (Thermo Fisher Scientific (Shanghai, China).

2.2. Extract preparation

The *Belamcanda chinensis* used in this study was identified as *Belamcanda chinensis* (L.) DC by Prof. Zhang Pengyue (Yunnan University of Chinese Medicine). *Belamcanda chinensis* was deposited in the herbarium of our institute with a voucher specimen (PGZ2021-9). *Belamcanda chinensis* slices were placed in a drying box until completely dry and crushed with a grinder and filtered through a 40 mesh sieve to obtain *Belamcanda chinensis* powder. In an Erlenmeyer flask, 30 g of the dried fine powder was dissolved in 270 mL of 70 % ethanol at a material-to-liquid ratio of 1:9 and subjected to ultrasonic extraction at room temperature for 1 h. After centrifugation, the filtrate was evaporated and concentrated in ethanol. *Belamcanda chinensis* ethanol extract was dissolved in 100 mL of double distilled water, followed by organic solvent extraction with 100 mL of dichloromethane. The resulting dichloromethane components were rotated, evaporated and concentrated into a dichloromethane extract, named BCE. For convenience, BCE in the manuscript refers to the *Belamcanda chinensis* alcohol-extracted dichloromethane extract phase. The BCE was dissolved in DMSO, using 0.22 μm micromembrane to filter out bacteria and impurities, and stored at −20 °C at a concentration of 100 mg/mL. The final DMSO concentration did not exceed 0.5 %.

Table 1
The primers for RT-qPCR.

gene	forward primer	reverse primer
Ras	5′-ACAGGCTCAGGACTTAGCAAGAA-3′	5′-TCCAGTCGGATGTCTACTCCTATG-3′
Raf	5′-TCCAGTCGGATGTCTACTCCTATG-3′	5′-TGATCTGATCTCGGTTGTTGATGT-3′
18S	5′-AAACGGCTACCACATCCAAG-3′	5′-CCTCCAATGGATCCTCGTTA-3′

2.3. Analysis of Belamcanda chinensis extract by gas chromatography-mass spectrometer (GC-MS)

The BCE sample was analyzed by using the Acquity GC-MS ISQ LT system (Thermo Fisher Scientific, USA). The TG-5MS capillary column was used to separate BCE samples. The oven temperature program was initially set to 60 °C and held for 5 min. It was then heated at a rate of 3.5 °C/min until reaching 100 °C, where it was maintained for another 5 min. Subsequently, the temperature was increased at a rate of 8 °C/min until reaching 200 °C, and again maintained for 5 min. Following this, the temperature was raised at a rate of 15 °C/min to reach 300 °C, which is then maintained for an additional 15 min with a solvent delay of 4 min. The operating parameters were as follows: the injection port and detector temperatures were 280 °C and 300 °C, respectively; quadrupole temperature was 280 °C; ion source temperature was 300 °C; electron impact ionization (EI) mode was set at 70 eV. Finally, the results were obtained from a full scan of the sample within a scanning range of 50–650m/z.

2.4. Cell culture

Human NSCLC cell lines SPC-A1 and NCI–H460 were kept in the laboratory and cultured in RPMI 1640 medium, to which FBS (10 %), penicillin (100 U/mL) and streptomycin (100 μg/mL) were added. HEK-293T (Human embryonic kidney 293 T) cells were kept in the laboratory and cultured in DMEM with FBS (10 %), streptomycin (100 μg/mL) and penicillin (100 U/mL). The cells were incubated at 37 °C in an incubator filled with 5 % CO_2.

2.5. Cell viability assay

Cell viability was measured by MTS assay. The drug concentration that resulted in IC_{50} (50 % inhibition of cell growth) was calculated by fitting the dose-response curve. The cells of SPC-A1, NCI–H460, and HEK-293T were cultured respectively in 96-well at a density of 5×10^3 cells in 100 μL per well and incubated at 37 °C for 12 h until the cells adhered to the plate for drug treatment. After cells were treated with BCE of different concentrations (0, 25, 50, 100, 200, 400 μg/mL) for 72 h, 20 μL of PMS and MTS mixture was added to each well (50 μL of PMS/1 mL of MTS). After incubation for additional 4 h, the optical density (490 nm) was determined using a microplate reader, and the IC_{50} value was calculated.

2.6. Analysis of cell cycle by flow cytometry

SPC-A1 and NCI–H460 cells were plated at a density of 1×10^5/mL and treated with BCE (0, 40, 80, 160 μg/mL) after the cells adhered to the plate. After 24 h of treatment, cells were collected and washed twice with PBS. The cells were dyed by adding 2 μL Cystain DNA 1 step (Partec GmbH, Münster, Germany) with 30 min at room temperature. The analytical statistics of the total cell population in the three different phases (G0/G1, S, G2/M) of the cell cycle was determined using FCS Express4.

2.7. Annexin V-FITC apoptotic assay

SPC-A1 and NCI–H460 cells were plated at a density of 1×10^5/mL and treated with BCE (0, 40, 80, 160 μg/mL) after the cells adhered to plate. After the drug treatment, the cells were collected and using Annexin V-FITC and propidium iodide (PI) to tint and analysis using a flow cytometer (Partec CyFlow R Space) and FloMax software version 2.

2.8. Reverse transcription-quantitative polymerase chain reaction (RT-qPCR)

The TRIzol reagent was used to isolate RNA from SPC-A1 and NCI–H460 cells, which cells have been added to BCE (0, 40, 80, 160 μg/mL for 24 h). RNA was reverse transcribed into cDNA using MMLV reverse transcriptase (Promega Corporation). Quantitative PCR was conducted on an ABI7000 cycler (Applied Biosystems; Thermo Fisher Scientific Inc.) using GoTaq qPCR Master Mix (Promega, Corporation) following the manufacturer's specification. The primer sequences used for RT-qPCR are listed in Table 1.

2.9. Western blot and cyto C extraction

SPC-A1 and NCI–H460 cells were treated with different concentrations (0, 40, 80 and 160 μg/mL) of BCE for 24 h or incubated with 160 μg/mL of BCE at 37 °C for 6, 12 and 24 h respectively, after which cells were collected and washed with PBS. The cells were lysed with a RIPA (radioimmunoprecipitation assay) buffer containing protease and phosphatase inhibitor cocktails. The sodium dodecyl sulfate-polyacrylamide gel electrophoresis (SDS-PAGE) was used to separate cell proteins, and transferred to nitrocellulose

Table 2
GC-MS analysis of the BCE.

NO	CAS#	Compound	Area (%)	Retention time(min)
1	124-07-2	Octanoic acid	0.34	18.05
2	334-48-5	n-Decanoic acid	1.16	26.71
3	121-33-5	Vanillin	0.71	27.01
4	498-00-0	4-Hydroxy-3-methoxybenzyl alcohol	0.43	28.35
5	498-02-2	Apocynin	5.86	29.07
6	2040-15-5	2,4,6-Trimethylpropiophenone	0.33	29.67
7	143-07-7	lauric acid	2.08	30.72
8	6627-88-9	Phenol,2,6-dimethoxy-4-(2-propenyl)-	1.05	31.17
9	57-10-3	n-Hexadecanoic acid	22.93	31.25
10	628-97-7	Hexadecanoic acid, ethylester	3.16	32.60
11	2553-19-7	Silane, diethoxydiphenyl-	0.32	33.00
12	124-10-7	Methyl tetradecanoate	0.56	33.19
13	544-63-8	Tetradecanoic acid	23.59	33.85
14	60-33-3	9,12-Octadecadienoic acid (Z,Z)-	4.38	38.58
15	112-84-5	13-Docosenamide, (Z)-	0.62	46.16
16	1447-88-7	hispidin	1.23	47.38
17	18085-97-7	Jaceosidin	5.24	48.08
18	548-74-3	4H-1-Benzopyran-4-one, 5,6-dihydroxy-2-(3-hydroxy-4 -methoxyphenyl)-3,7-dimetho xy-	19.22	50.01
19	83-47-6	ç-Sitosterol	0.60	51.40
20	4723-32-4	11H-Dibenzo[b,e] [1,4]dioxepi n-7-carboxylic acid, 3,8-dimethoxy-1,4,6,9-tetrame thyl-11-oxo-, methyl ester	6.19	52.11

membranes. Immunostaining was performed with appropriate primary antibody, followed by horseradish peroxidase conjugated secondary antibody. The chemiluminescence reagent was used to detect the antibodies. Cytosolic proteins were extracted using digitonin buffer for the detection of CytoC by western blotting.

2.10. Fluorescence bimolecular complementary analysis between Ras and Raf

pBiFC-VC155 (#22011; Addgene) and pBiFC-VN155 (I152L) (#27097; Addgene) were used for fluorescence bimolecular complementary analyses. Ras and Raf expression vectors were purchased from Sangon Biotech (Shanghai, China). The Ras-Vc155 and Raf-Vn155 expression vectors were constructed using standard molecular cloning methods with restriction enzymes and T4 ligases. At a cell density of 1×10^5/mL, Ras-Vc155 and Raf-Vn155 vectors were transfected into HEK-293T cells using Lipofectamine 2000. After HEK-293T cells treated with BCE of different concentrations (0, 50, 100, 200, 400 μg/mL) for 48 h, fluorescence microscopy and reader were used to observe the bimolecular fluorescence complementary signal, respectively.

2.11. Nude mouse xenograft tumor model

Animal experiment had been approved by the Experimental Animal Ethics Committee of Kunming University of Science and Technology and complied with the guidelines of the United States (NIH publication #85-23, revised in 1985). Fourteen male *nu/nu* BALB/c mice (approximately 16 g) were purchased from Shanghai SLAC Laboratory Animals (Shanghai, China). The mice were kept in a barrier facility with a 12-h light-dark cycle, and food and water were freely available. A mouse xenograft model was established by inoculating of 1.5×10^7 SPC-A1 cells subcutaneously (s.c.) on the both flanks of five-week old BALB/c nude mice [38]. The mice were randomized into control and treatment groups of seven animals each when the xenografts were palpable, with an average size of ~50 mm^3. Control (castor oil) or drug (240 mg/kg of BCE dissolved in castor oil) was administered by intraperitoneal injection (i.p.) once every two days. During the experiment, if the mice did not eat or drink water within 24–48 h, resulting in significant weight loss or dehydration, the humane endpoint was considered, and the mice were euthanized. After 15 days of treatment, we used carbon dioxide (45 % volume displacement/min) inhalation to anesthetize the mice, waited until they were fully anesthetized, and euthanized them by cervical dislocation. Tumor size and body weight were measured daily. Vernier caliper was used for tumor size measurement, and the following formula: length × $width^2$ × 0.4 (width is the smallest diameter, and length is the diameter perpendicular to the width) was used for tumor volumes calculation. After the mice were sacrificed, tumors were collected, weighed, and photographed. The expression levels of Ras, Raf, p-Akt, and Akt proteins in the tumor tissue were detected by western blotting.

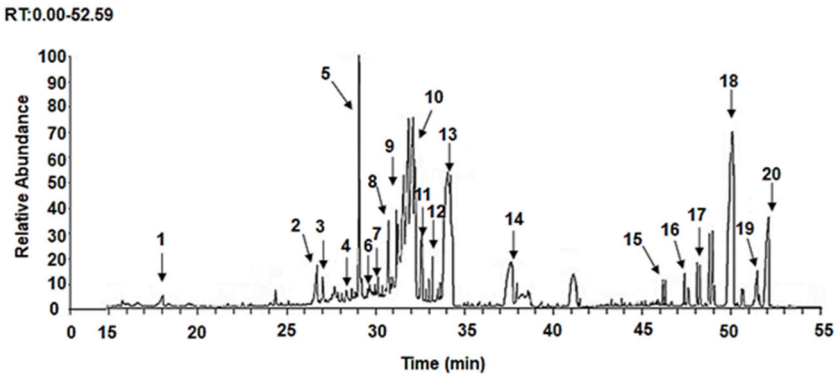

Fig. 1. GC-MS chromatogram of the BCE.

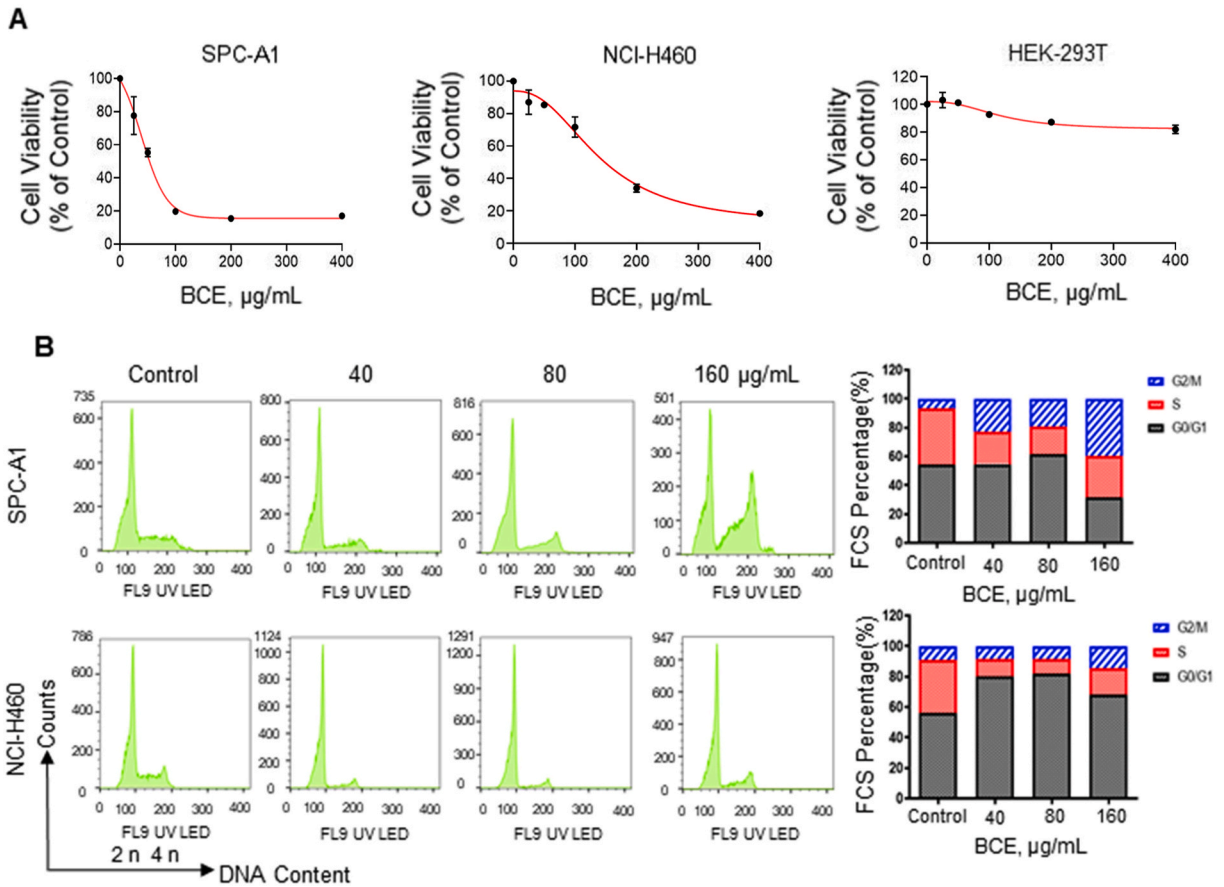

Fig. 2. The effect of BCE on the viability and cell cycle distribution of NSCLC cells. (A) HEK-293T, SPC-A1, and NCI–H460 cells were seeded in 96-well plates at a density of 5×10^3/well and treated with various concentrations (control (0), 25, 50, 100, 200, 400 μg/mL) of BCE for 72 h, and cell viability was examined by MTS assay. (B) BCE triggered cell cycle arrest in NSCLC cells. SPC-A1 and NCI–H460 cells were exposed to different concentrations of BCE (control (0), 40, 80, 160 μg/mL) for 24 h. Then, the cells were stained with PI and the cell cycle distribution was analyzed by flow cytometry.

2.12. Statistical analysis

All data are expressed as the mean ± SD (standard error) obtained from at least three independent experiments. The statistical analyses between the two groups were conducted using an unpaired *t*-test. Multiple comparisons using one-way analysis of variance (ANOVA) were performed, followed by Tukey's post hoc ANOVA test. $P < 0.05$ has statistical significance.

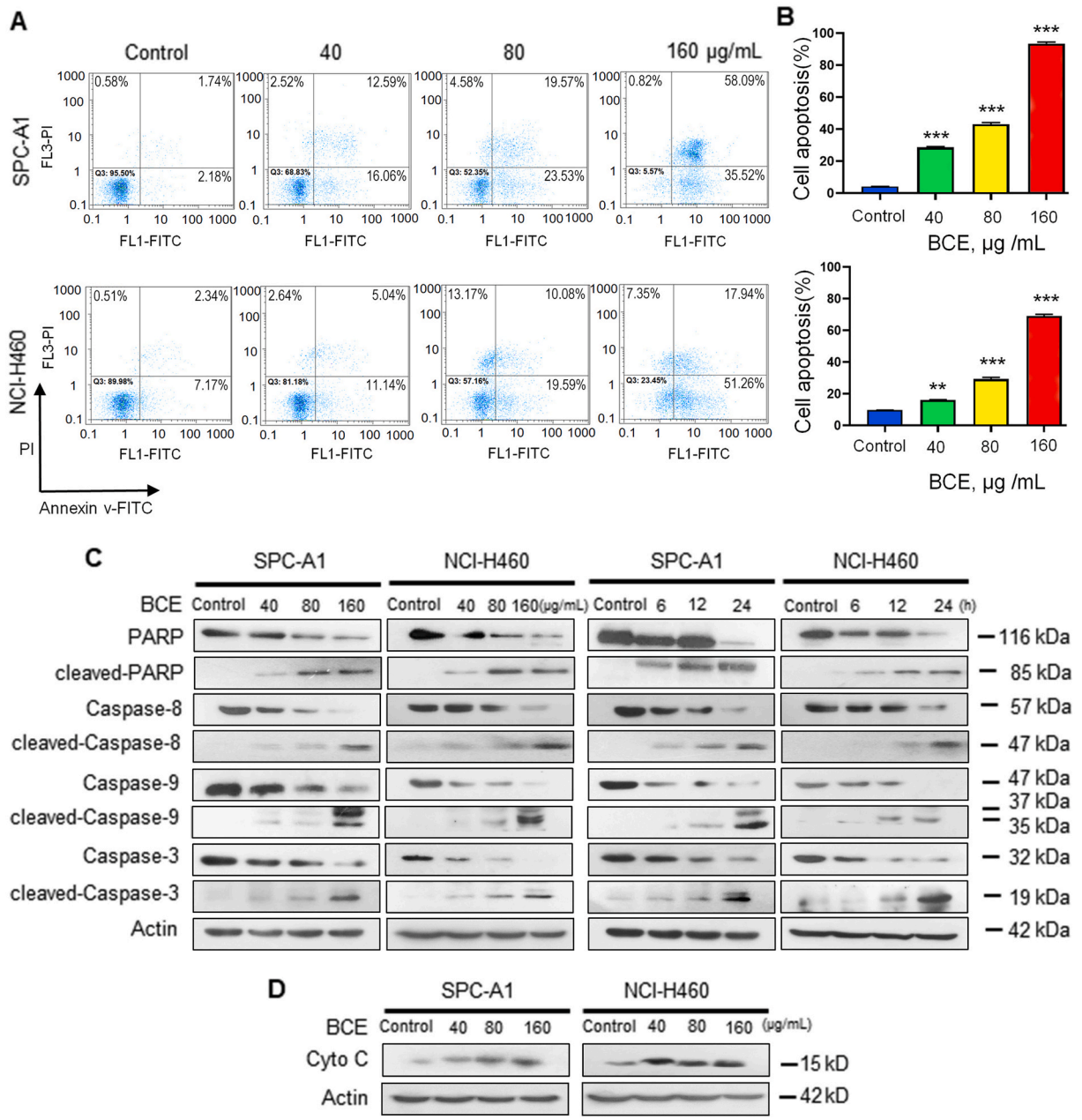

Fig. 3. BCE activated apoptosis pathways in NSCLC cells. (A) After treating NSCLC cells with various concentrations of BCE (control (0), 40, 80, 160 μg/mL) for 24 h, apoptotic cells were detected by flow cytometry after double staining with AnnexinV-FITC and PI. (B) Statistical analysis of apoptosis rates through three independent experiments. **, $P < 0.01$; ***, $P < 0.001$; one-way ANOVA, post hoc comparisons, Tukey's test. Columns, mean; error bars, SE. (C) BCE led to specific cleavage of PARP and Caspases. NSCLC cells SPC-A1 and NCI–H460 were exposed to escalating concentrations (control (0), 40, 80, 160 μg/mL) of BCE for 24 h or to 160 μg/mL of BCE for various times (control (0), 6, 12, 24 h). Thereafter, PARP and Caspases were examined by Western blot. (D) BCE induced Cyto C release. NSCLC cells were treated with different concentrations of BCE for 24 h, and Cyto C in the cytosolic fraction was measured by Western blot. Figs. 3C and 4A were the same experiment setting, and the Actin bands in Figs. 3C and 4A were the same.

3. Results

3.1. Components identification of BCE by GC-MS analysis

To identify the compounds, BCE was examined using GC-MS. The GC-MS results showed that BCE contained more than 20 components, with an elution time of approximately 18.05–52.11 min (Table 2 and Fig. 1). Chemical composition record based on the

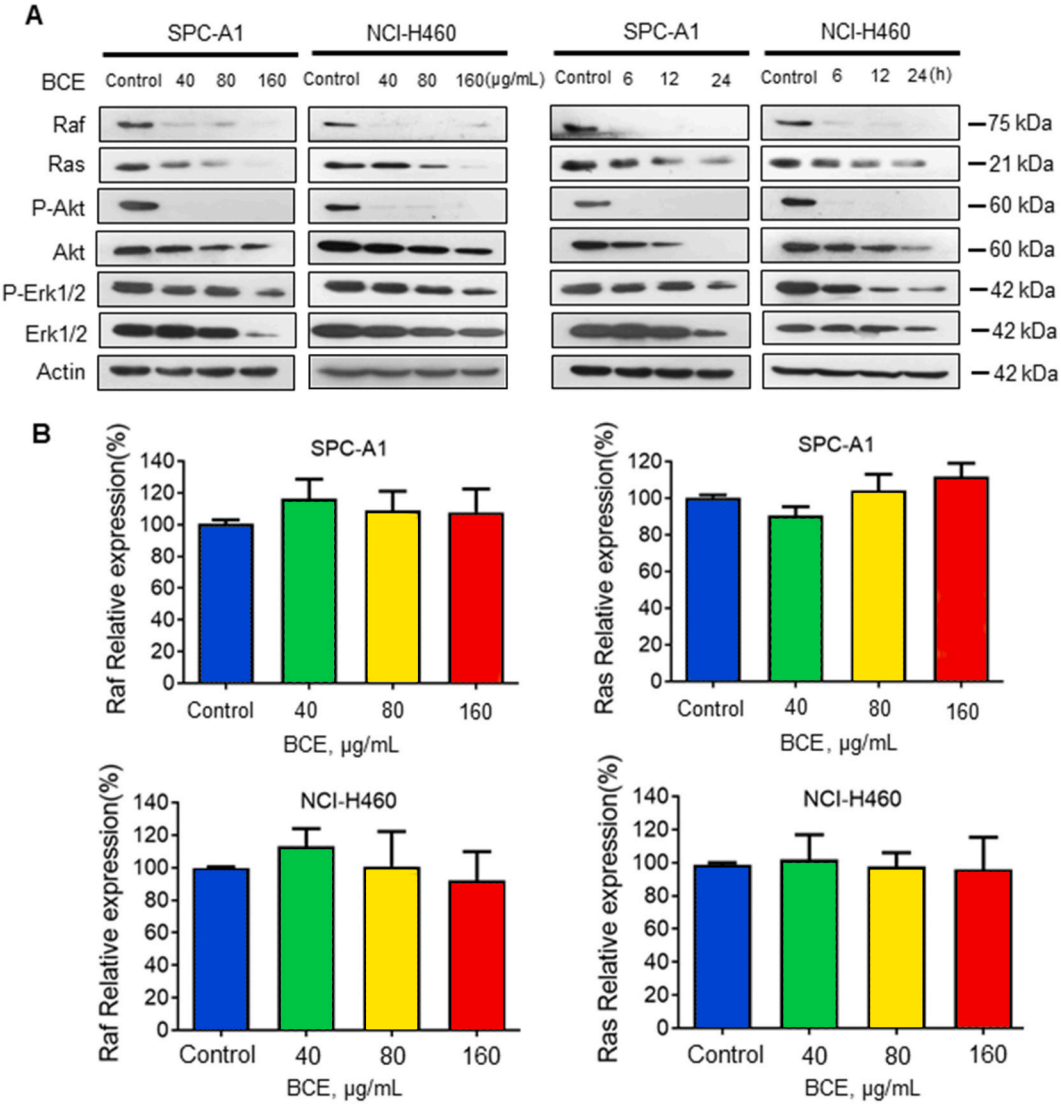

Fig. 4. Effect of BCE on MAPK (Ras/Raf) and Akt signaling pathways in SPC-A1 and NCI–H460 cells. (A) SPC-A1 and NCI–H460 cells were exposed to various concentrations of BCE (control (0), 40, 80, 160 μg/mL) for 24 h, or to 160 μg/mL of BCE at different times (control (0), 6, 12, 24 h). MAPK (Ras/Raf) and Akt signaling pathway proteins were analyzed by Western blot. (B) NSCLC cells were treated with different concentrations of BCE (control (0), 40, 80, 160 μg/mL) for 24 h. Raf and Ras gene transcription levels were evaluated by RT-qPCR. Figs. 3C and 4A were the same experiment setting, and the Actin bands in Figs. 3C and 4A were the same.

relative retention time and mass spectrometry with real samples and/or NST/NBS and Wiley library the comparison of the spectrum (Table 2).Some peaks, such as those at the elution times of 41 and 49 min, were not identified by the libraries; therefore, no specific substances were identified and will be studied in the future. Most identified compounds were octadecanoic acid and its derivatives, whereas a few were flavonoids.

3.2. Effect of BCE on the viability of NSCLC cells SPC-A1 and NCI–H460

The anti-proliferative effect of BCE was evaluated in NSCLC cells SPC-A1 and NCI–H460 treated with increasing concentrations of BCE (0, 25, 50, 100, 200, 400 μg/mL). BCE significantly decreased the viability of SPC-A1 and NCI–H460 cells (Fig. 2A). Additionally, the inhibitory effect of BCE on the SPC-A1 cells is better than that of NCI–H460 cells, with IC_{50} values of 46.6 μg/mL and 126.7 μg/mL, respectively. However, no significant effect on cell viability was observed when normal HEK-293T cells were treated with BCE (Fig. 2A).

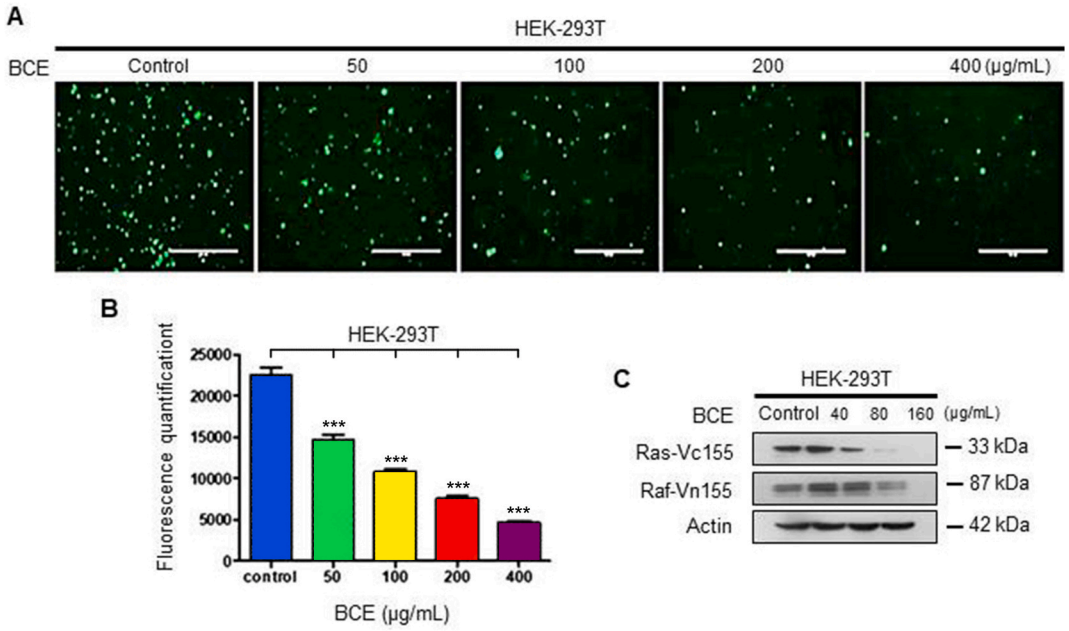

Fig. 5. Effect of BCE on Ras/Raf mediated by fluorescence bimolecular complementary. (A) After transfection of HEK-293T cells with bimolecular fluorescence complementary vectors Ras-Vc155 and Raf-Vn155 and treatment with gradually increasing concentration of BCE (control (0), 50, 100, 200, 400 μg/mL) for 48 h, fluorescence microscopy was used to observe the bimolecular fluorescence complementary signal. (B) Fluorescence signal reader was used to detect the fluorescence signal in (A). Statistical analysis of fluorescence quantification through three independent experiments. ***, $P < 0.001$, one-way ANOVA, post hoc comparisons, Tukey's test. Columns, mean; error bars, SE. (C) HEK-293T cells were transfected with Ras-Vc155 and Raf-Vn155 vectors and treated with gradually increasing concentration of BCE (control (0), 40, 80, 160 μg/mL) for 48 h. Thereafter, Western blot was used to detect the expression levels of Ras-Vc155 and Raf-Vn155 proteins.

3.3. Effect of BCE on cell cycle distribution of NSCLC cells SPC-A1 and NCI–H460

To study the mechanism underlying the anti-growth effect of BCE on SPC-A1 and NCI–H460 NSCLC cells, the cell cycle distribution of NSCLC cells after BCE treatment was determined by flow cytometry. The results showed that BCE can induce the cell cycle arrest of NCI–H460 cells in G1 phase by treated with different concentrations (0, 40, 80 and 160 μg/mL) of BCE for 24 h, which the proportions of G1 phase were 55.84 %, 80.27 %, 81.96 % and 68.22 % (Fig. 2B). For SPC-A1 cells, BCE blocked the cell cycle in G2/M phase after exposed to different concentrations (0, 40, 80 and 160 μg/mL) of BCE for 24 h. The proportion of cells in the G2/M phase was 6.55 %, 22.71 %, 19.56 %, and 39.87 %, respectively (Fig. 2B). The results demonstrated that BCE can effectively induce NSCLC cell lines SPC-A1 and NCI–H460 cell cycle arrest in concentration-dependent manner.

3.4. BCE induces apoptosis in NSCLC cells SPC-A1 and NCI–H460

Furthermore, to determine whether BCE induces apoptosis in NSCLC cells, SPC-A1 and NCI–H460 cells were exposed to BCE at concentrations of 0, 40, 80 and 160 μg/mL for 24 h, respectively. After treating cells with BCE and staining with propidium iodide (PI) and Annexin V-FITC, the apoptosis rate was measured using flow cytometry. The results demonstrated that the apoptosis rates of SPC-A1 and NCI–H460 cells treated with BCE were concentration-dependent (Fig. 3A and B). Namely, the apoptosis rates of SPC-A1 cells treated with BCE at 40, 80 and 160 μg/mL were 28.65 %, 53.1 % and 93.61 %, respectively (Fig. 3A and B), while the apoptosis rates of NCI–H460 cells treated with corresponding concentrations of BCE were 16.18 %, 29.67 % and 69.2 %, respectively (Fig. 3A and B).

3.5. BCE activates the apoptosis pathway in NSCLC cells SPC-A1 and NCI–H460

To further understand the molecular mechanism underlying BCE-induced apoptosis in SPC-A1 and NCI–H460 NSCLC cells, we examined the expression of apoptosis-related proteins. The data demonstrated that BCE promoted the specific cleavage of PARP, Caspase-3, -8, and -9, and upregulated the levels of cleaved caspases and cleaved PARP in a time- and dose-dependent manner; and induced apoptosis in NSCLC cells (Fig. 3C). In addition, when mitochondria are unstable, Cyto C is transferred from the mitochondria to the cytosol; therefore, Cyto C content in the cytosolic fraction was measured. As the concentration of BCE increased, cytosolic Cyt C content gradually increased (Fig. 3D). The changes in the apoptotic proteins mentioned above are consistent with the results of flow cytometry (Fig. 3A and B) in detecting apoptosis of SPC-A1 and NCI–H460 cells, and at the protein molecular level, a reasonable explanation has been provided for the exogenous and endogenous apoptotic pathways of NSCLC cells induced by BCE.

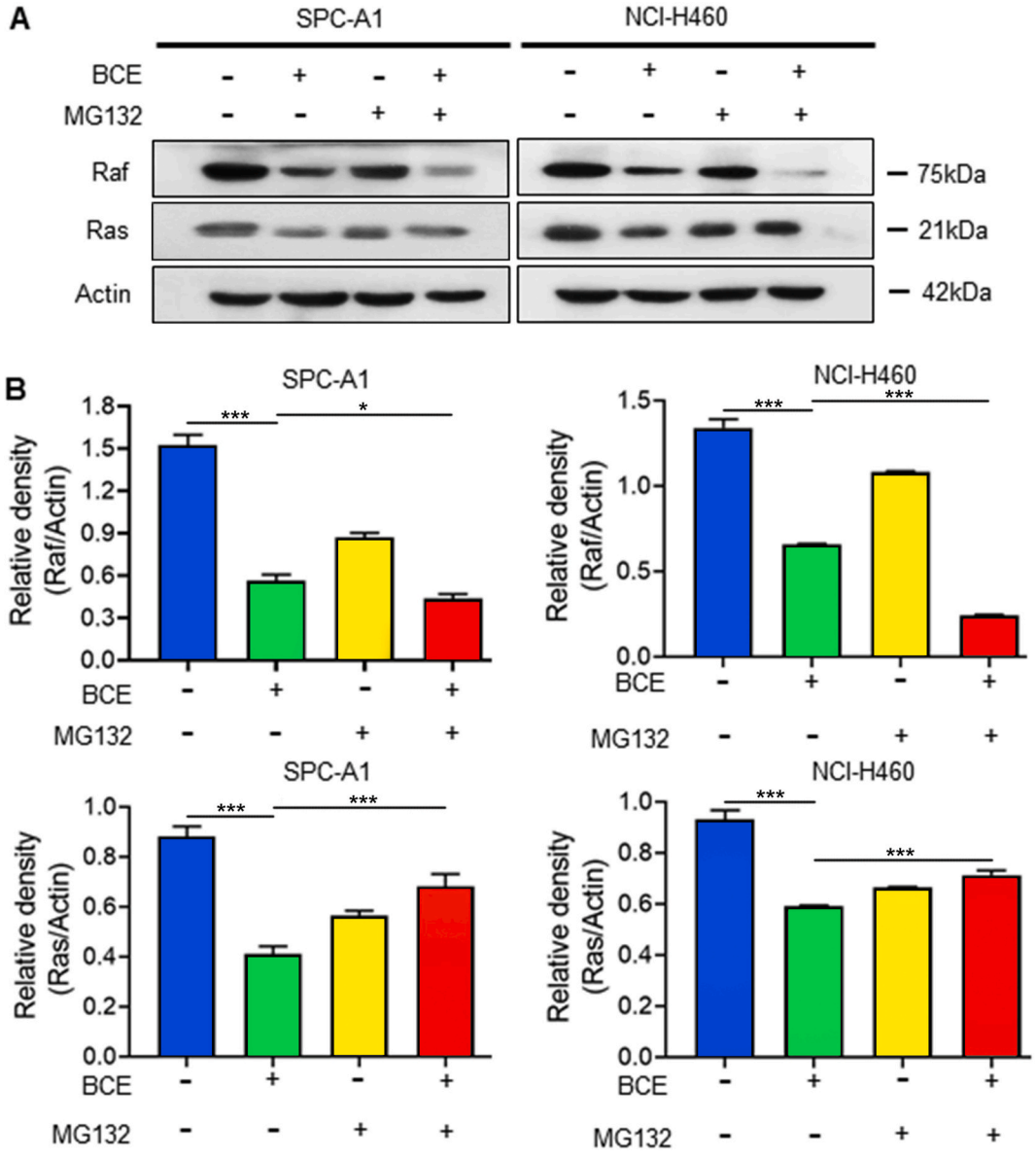

Fig. 6. Effect of BCE on the stability of Ras and Raf in proteasome pathway. (A) Western blot was used to detect the combining effects of MG132 (10 μM) and BCE (80 μg/mL) on Ras and Raf proteins in NSCLC cells SPC-A1 and NCI–H460 for 24 h. (B) Analysis of the relative density of Ras and Raf proteins in (A). Statistical analysis of band signal through three independent experiments. *, $P < 0.05$; ***, $P < 0.001$, one-way ANOVA, post hoc comparisons, Tukey's test. Columns, mean; error bars, SE.

3.6. BCE abrogates MAPK (Ras/Raf) and Akt pathway in NSCLC cells SPC-A1 and NCI–H460

Considering the importance of the Akt and MAPK (Ras/Raf) signaling pathways in the regulation of cell proliferation, these pathways may be the mechanisms underlying the antitumor effects of BCE. We detected the expression levels of proteins in the Akt and MAPK (Ras/Raf) pathways and evaluated the effect of BCE on the transcriptional levels of Ras and Raf in SPC-A1 and NCI–H460 NSCLC cells. The results showed that BCE reduced the expression of Ras, Raf, p-Erk1/2, and p-Akt proteins in a dose- and time-dependent manner (Fig. 4A). Similarly, the expression of total Erk1/2 and total Akt were reduced in a time- and dose-dependent manner (Fig. 4A). However, it had no effect on the transcription levels of the Ras and Raf genes (Fig. 4B).

3.7. BCE blocks the bimolecular fluorescence complementarity mediated by Ras and Raf

To clarify whether BCE blocks the binding of Ras and Raf proteins, Venus fluorescence bimolecular complementary (Vc155/Vn155)

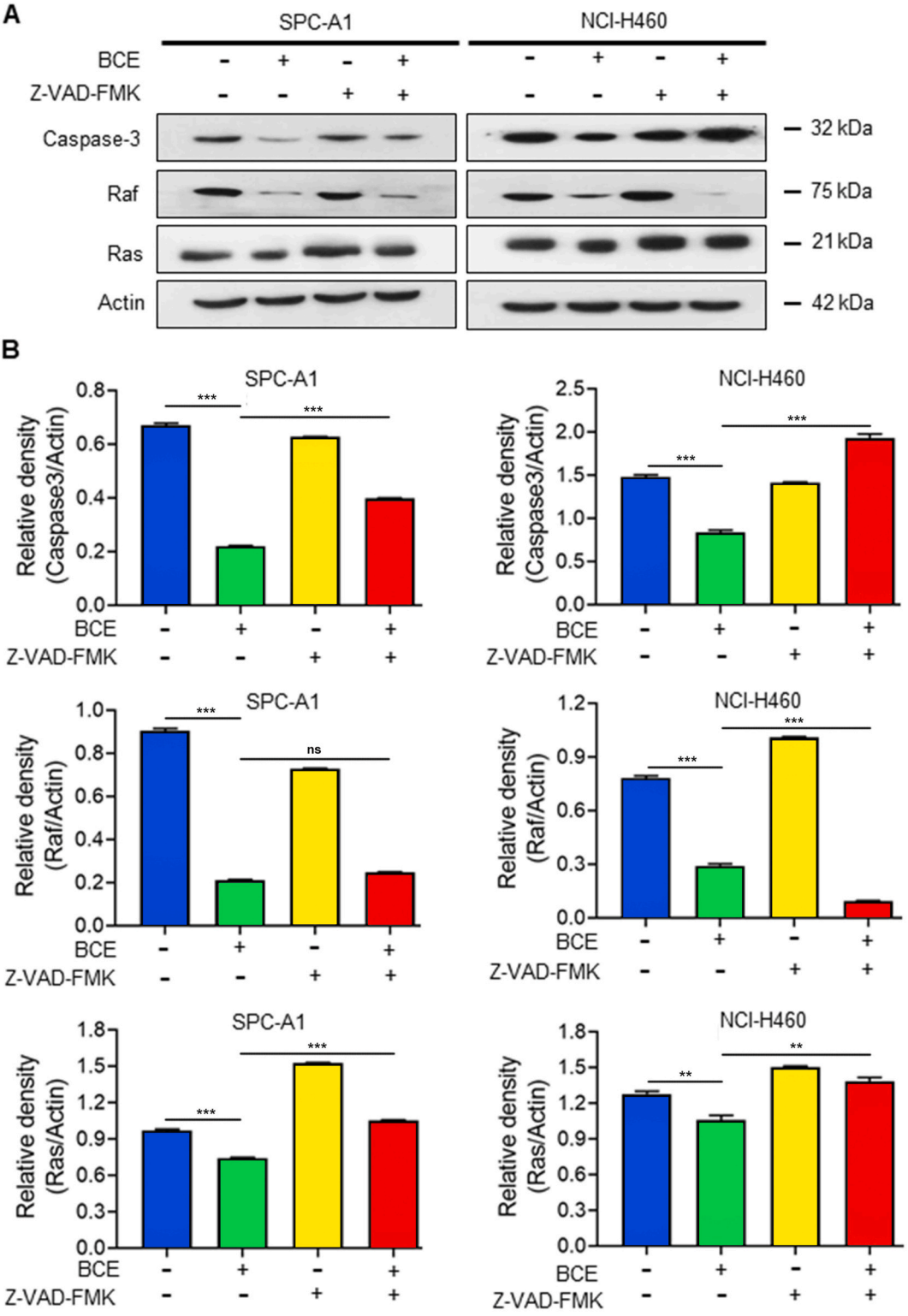

Fig. 7. Effect of BCE on the expression of Ras and Raf through apoptosis pathway. (A) After treatment with Z-VAD-FMK (40 μM) or BCE (80 μg/mL) for 24 h, or both, the expression of Ras and Raf proteins were detected by Western blot in NSCLC cells SPC-A1 and NCI–H460. (B) Analysis of the relative density of Caspase-3, Ras and Raf proteins in (A). Statistical analysis of band signal through three independent experiments. ns, no significance; **, $P < 0.01$; ***, $P < 0.001$, one-way ANOVA, post hoc comparisons, Tukey's test. Columns, mean; error bars, SE.

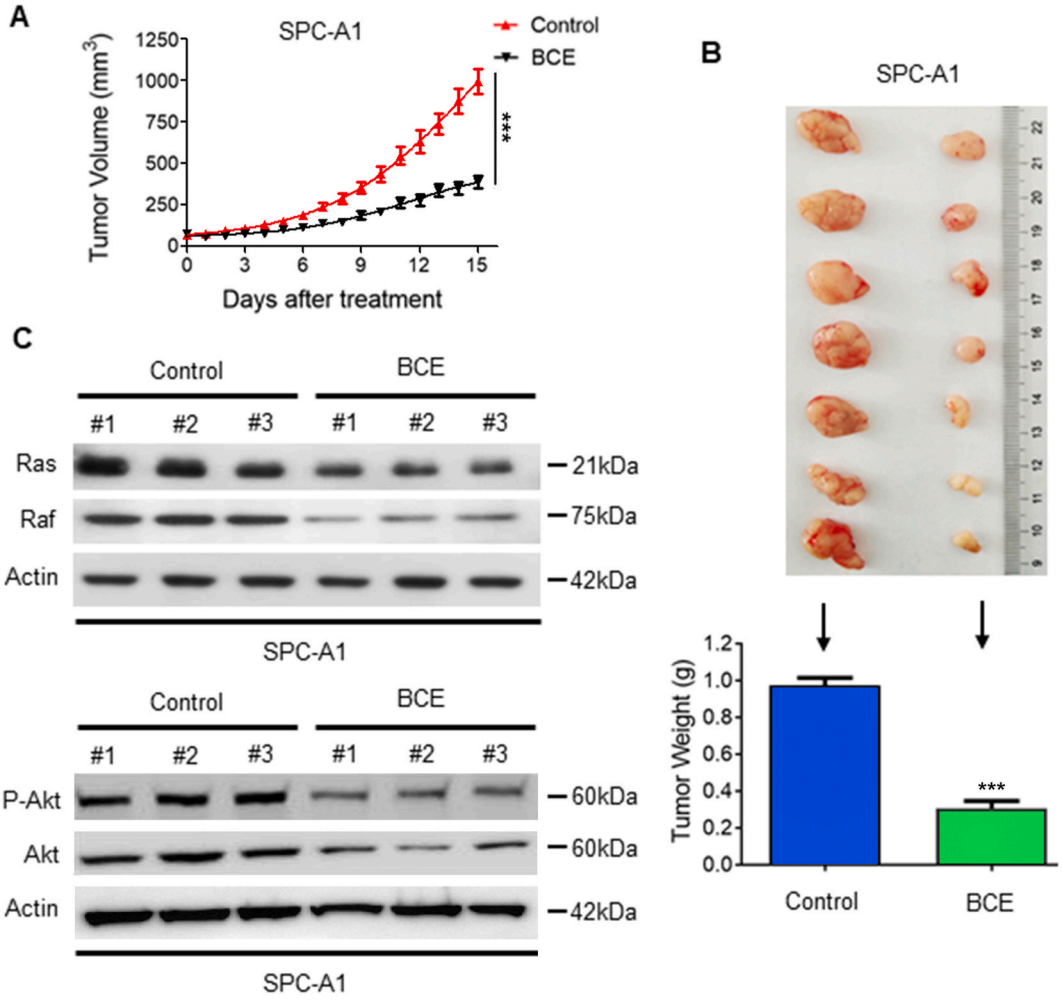

Fig. 8. BCE inhibited the growth of subcutaneous xenografts of SPC-A1 cells in nude mice. (A) The growth curves of subcutaneous xenografts of SPC-A1 cells are shown. The measured tumor size is plotted against the number of days after initiation of BCE treatment. ***, $P < 0.001$; Comparisons between the two groups were made using the student's *t*-test. (B) Representative photographs and average weight of tumors isolated after sacrifice of mice. ***, $P < 0.001$; the student's *t*-test. (C) The expression of Ras, Raf, Akt and p-Akt proteins in xenograft tumors after BCE treatment was detected by western blotting.

vectors mediated by Ras and Raf were constructed and the inhibitory effect of BCE on the binding of Ras and Raf was studied. Venus fluorescent proteins are divided into amino-(Vn155) and carboxyl-terminal (Vc155) segments. The binding of Ras and Raf reconstructs the Venus protein and emits fluorescence signals. As the concentration of BCE increased, the Venus fluorescence complementary signal was significantly downregulated (Fig. 5A and B). In addition, BCE downregulated the expression levels of Ras and Raf exogenously transfected with Venus fragments Vc155 and Vn155 tags in HEK-293T cells, respectively (Fig. 5C).

3.8. The molecular mechanisms of BCE degrades the Ras and Raf proteins

Furthermore, we were promoted to shed light on the degradation mechanism of Ras and Raf mediated by BCE. As shown in Fig. 6, the combined effects of the proteasome inhibitors MG132 and BCE on SPC-A1 and NCI–H460 cells were investigated. The results demonstrated that MG132 reversed the degradation of Ras protein by BCE (Fig. 6A and B). In contrast, the degradation of Raf protein by BCE was not reversed by the proteasome inhibitor MG132 (Fig. 6A and B). We also investigated whether the degradation of Ras and Raf was related to the apoptotic pathway in SPC-A1 and H460 cells. The combined effects of the Caspase-3 inhibitor (Z-VAD-FMK) and BCE on Ras and Raf proteins in NSCLC cells were investigated. Under the conditions in which Z-VAD-FMK inhibited the degradation of the Caspase-3 protein (Fig. 7A and B), the expression levels of Ras and Raf proteins by BCE treatment were detected by Western blot. The result demonstrated that the degradation of the Ras protein by BCE was inhibited by Z-VAD-FMK in SPC-A1 and H460 cells (Fig. 7A and B). In contrast, the degradation of Raf protein by BCE was not reversed by Z-VAD-FMK treatment (Fig. 7A and B).

3.9. BCE abrogates the growth of xenografted NSCLC cells in nude mice

To determine whether BCE inhibited the growth of NSCLC cells *in vivo*, SPC-A1 cells were injected subcutaneously on the flanks of five week-old BALB/c male nude mice. When the tumor size reached approximately 50 mm^3, the control group (castor oil) or the BCE treatment group (240 mg/kg BCE) were administered an intraperitoneal injection once every two days for 15 days. Our preliminary experiments demonstrated that the animal was very well tolerated a concentration of 240 mg/kg. Fig. 8A shows a tumor growth curve of change over time. BCE effectively inhibited the growth of SPC-A1 tumors. Tumor size was significantly reduced in the BCE treatment group compared to the control group (Fig. 8B, top). In addition, tumor weight was significantly lower in the BCE-treated group than in the control group (Fig. 8B, bottom). Western blotting was used to detect the protein expression of Ras, Raf, Akt and p-Akt in tumor tissues. As shown in Fig. 8C, BCE significantly inhibited the expression of Ras, Raf, Akt, and p-Akt *in vivo*. In animal experiment, the weight of mice was stable, and no significant difference between the control group and the treatment group was found. These mice showed normal eating behavior and movement, and no mice died.

4. Discussion

Lung cancer is a common malignant tumor with poor prognosis, which poses a serious threat to public health [39]. Although great advance has been achieved in the treatment of NSCLC over the past decades, the prognosis of patients with high stage NSCLC is poor [40–42]. Therefore, it is urgent to find drugs with low toxicity against NSCLC. The use of TCM for antitumor treatment has the advantages of good curative effects and low toxic side effects [29,30]. Many TCM extracts have demonstrated good *in vivo* and *in vitro* anti-lung cancer effects [43–46]. *Belamcanda chinensis* is a major anticancer ingredient in TCM. Previously studies have documented the antitumor activity of *Belamcanda chinensis* in several tumor types [33–37], and its antitumor mechanisms include inducing cell cycle arrest, downregulating mitochondrial potential, and producing excessive reactive oxygen species to activate the mitochondrial apoptosis pathway and caspase cascade [33–37,47].

The anti-tumor effect of BCE in the NSCLC cell lines SPC-A1 and NCI–H460 was investigated. The results showed that BCE inhibited the proliferation and induced apoptosis of SPC-A1 and NCI–H460 NSCLC cells. Moreover, the *in vivo* anti-proliferative potential of BCE in transplanted SPC-A1 cells in nude mouse xenograft models was studied. The main strategies for treating cancer were inhibition of cell proliferation and apoptosis induction. In this study, the inhibitory effect of BCE on the viability of NSCLC cells SPC-A1 and NCI–H460 and its blocking effect on the G1 phase of the NCI–H460 cell cycle and the G2/M phase of SPC-A1 cells indicate that BCE has anti-proliferative effects on NSCLC cells *in vitro*. However, the mechanism by which BCE blocks the cell cycle of NSCLC cells remains unclear, and whether BCE can regulate the cell cycle-related proteins CDKs and CDKI (a CDK inhibitor) needs to be further clarified. In addition, the *in vitro* anti-NSCLC effects of BCE are exerted by the induction of apoptosis. Apoptosis is caused by the activation of caspases. Caspase-9 is a key protein in the endogenous mitochondrial apoptosis pathway, while Caspase-8 is a key protein in the exogenous death receptor apoptosis pathway [48,49]. In this study, the specific cleavage of Caspase-8, 9, 3 and PARP induced by BCE, as well as the release of Cyto C from the mitochondria to the cytosol, promoted the apoptosis in SPC-A1 and NCI–H460 NSCLC cells. It can be concluded that BCE-mediated apoptosis of SPC-A1 and NCI–H460 NSCLC cells is achieved through the activation of the endogenous mitochondrial apoptosis pathway and exogenous death receptor pathway.

Moreover, the Ras/Raf/MEK/ERK pathway has been thought as a promising target for cancer treatment [50–52], indicating that Ras exerts an vital role in the activation of the phosphatidylinositol 3-kinase (PI3K/Akt) pathway and regulates various substrates [39,53,54]. This study provides evidence that BCE effectively inhibits NSCLC cell growth *in vivo* and *in vitro* by inhibiting the PI3K/Akt and Ras/Raf signaling pathways and inhibiting NSCLC cell growth in a xenograft model. The analysis revealed that the binding of Ras and Raf proteins was inhibited by treatment with BCE, and the downregulation of Ras by BCE was not caused by the suppression of Ras gene transcription levels in SPC-A1 and NCI–H460 NSCLC cells, but by the influence of proteasome degradation and apoptosis pathways, as both the pan-caspase inhibitor Z-VAD-FMK and the proteasome inhibitor MG132 can block Ras degradation induced by BCE. However, proteasome degradation and apoptotic pathways were not the reasons for the degradation of Raf protein by BCE treatment in SPC-A1 and NCI–H460 NSCLC cells, and further investigation is needed. BRAF mutations, particularly BRAFV600 mutations, are found in cancers, including colorectal cancer, melanoma, thyroid cancer, and non-small cell lung cancer, and are thought to cause malignancy [55,56]. Inhibitors targeting BRAF mutations, such as Vemurafenib and Dabrafenib, have been developed to treat these tumors and have achieved good therapeutic results [57]. In this study, BCE efficiently reduced the expression of Raf, suggesting the potential use of BCE in patients with tumors, especially those harboring BRAF mutations as driving oncogenes, such as BRAFV600E bearing non-small cell lung carcinoma and melanoma patients, or in combination with other oncogene inhibitors such as MEK inhibitors Trametinib and Binimetinib. Compared with RAF inhibitor monotherapy, MEK inhibitor combination therapy is more effective and improves progression free survival and overall survival [58]. Therefore, whether BCE exerts antitumor effects in combination with MEK inhibitors in BRAFV600 mutation-bearing melanoma or NSCLC cells requires further clarification. In addition, GC-MS analysis revealed that BCE contains more than 20 compounds, most of which are fatty acids, but also flavonoids and other compounds. Of these 20 compounds, the flavonoids jaceosidin [59] and hispidin [60], as well as other compounds including vanillin [61], apocynin [62], lauric acid [63], and gamma-sitosterol [64], have been shown to have antitumor activity in a variety of cancers, including non-small cell lung cancer. Therefore, we speculated that the pharmacologically active substances in BCE against NSCLC cells, SPC-A1 and NCI–H460, may be its constituent compounds. However, the anti-NSCLC effects and mechanisms of the compounds present in BCE require further clarification, especially to determine which compounds can downregulate Raf protein expression.

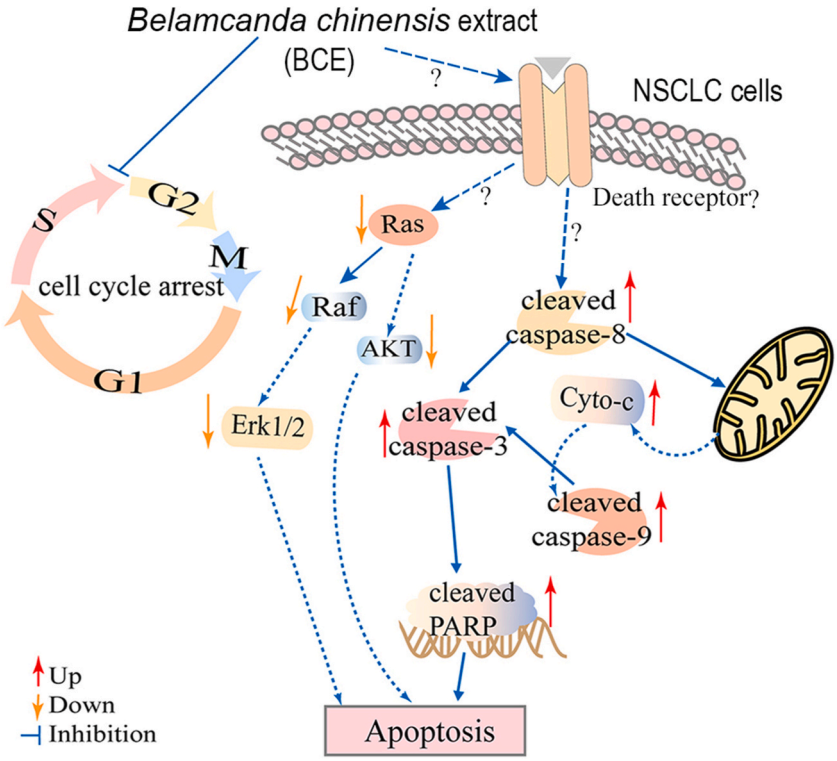

Fig. 9. Molecular mechanism of BCE inhibiting proliferation and inducing apoptosis of NSCLC cells.

5. Conclusions

Owing to the high morbidity and mortality associated with NSCLC, it is urgent to identify effective therapeutic drugs. We prepared a dichloromethane extract of the traditional Chinese medicine *Belamcanda chinensis* (BCE) and investigated its anti-NSCLC effects and mechanisms of action. The results demonstrated that BCE significantly induced cell cycle arrest, inhibited the proliferation of NSCLC cells *in vivo* and *in vitro*, and finally induced NSCLC cell apoptosis through endogenous mitochondrial and exogenous death receptors pathways (Fig. 9). This is expected to be further studied and used in the clinical treatment of patients with NSCLC. As far as we know, it is the first study to report that *Belamcanda chinensis* exerts anticancer effects in NSCLC cells by targeting Ras/Raf and inducing its degradation. The molecular mechanism of Ras degradation by BCE is related to the proteasome and apoptosis pathways; however, Raf degradation is not, and further clarification is needed. Moreover, the significant downregulation of the Raf protein by BCE suggests its potential application in cancer patients with BRAF mutations, particularly in NSCLC or melanoma with BRAFV600E mutations. In addition, phytochemical analysis revealed 20 major compounds in BCE; however, the anti-NSCLC effects of these compounds require further clarification. Moreover, there is an urgent need to identify the natural monomers that downregulate Raf in BCE compounds.

Funding

This research was funded by the Project of Yunnan Clinical Research Center for Geriatric Diseases (opening grant no. 2022YJZX-LN19; 2023YJZX-LN12; 202102AA310069; 2023YJZX-LN21), Basic Research Project of Yunnan Province (202401AT070358) and the Yunnan Province Dong Birong expert Workstation Project (grant no. 202105AF150032).

Ethics approval and consent to participate

The animal experiments in this study were approved by Experiment Animal Ethics Committee of Kunming University of Science and Technology with the number of No.01245.

Data availability statement

Data included in article/supp. material/referenced in article.

CRediT authorship contribution statement

Chong Ma: Writing – original draft, Software, Methodology, Investigation, Formal analysis, Conceptualization. **Jingyi Yin:** Writing – original draft, Software, Methodology, Investigation, Formal analysis. **Xiao Feng:** Writing – original draft, Software, Methodology, Investigation, Formal analysis. **Xin Wang:** Validation, Formal analysis, Data curation. **Xiaodie Cao:** Validation, Formal analysis, Data curation. **Chen Zhang:** Validation, Formal analysis, Data curation. **Rongjie Cui:** Validation, Formal analysis, Data curation. **Jingru Wei:** Validation, Formal analysis, Data curation. **Xu He:** Validation, Formal analysis, Data curation. **Yan Li:** Writing – review & editing, Validation, Supervision, Project administration, Funding acquisition, Conceptualization. **Li Chen:** Writing – review & editing, Validation, Supervision, Project administration, Funding acquisition, Conceptualization.

Declaration of competing interest

The authors declare that they have no known competing financial interests or personal relationships that could have appeared to influence the work reported in this paper.

Acknowledgements

Some experiments were performed in the Laboratory of Basic Medicine, Medical School, Kunming University of Science and Technology. Thanks for the Laboratory.

Appendix A. Supplementary data

Supplementary data to this article can be found online at https://doi.org/10.1016/j.heliyon.2024.e36032.

References

[1] F.R. Hirsch, G.V. Scagliotti, J.L. Mulshine, R. Kwon, W.J. Jr Curran, Y.L. Wu, L. Paz-Ares, Lung cancer: current therapies and new targeted treatments, Lancet 389 (10066) (2017) 299–311.
[2] F. Bray, J. Ferlay, I. Soerjomataram, R.L. Siegel, L.A. Torre, A. Jemal, Global cancer statistics 2018: GLOBOCAN estimates of incidence and mortality worldwide for 36 cancers in 185 countries, CA Cancer J Clin 68 (6) (2018) 394–424.
[3] World Health Organization, International Agency for Research on Cancer. Cancer Today. https://gco.iarc.who.int/media/globocan/factsheets/cancers/15-trachea-bronchus-and-lung-fact-sheet.pdf.
[4] H. Sung, J. Ferlay, R.L. Siegel, Global cancer statistics 2020: GLOBOCAN estimates of incidence and mortality worldwide for 36 cancers in 185 countries, CA Cancer J Clin 71 (3) (2021) 209–249.
[5] R. Siegel, K.D. Miller, A. Jemal, Cancer statistics 2020, CA Cancer J Clin. 70 (1) (2020) 7–30.
[6] T. Pearman, Psychosocial factors in lung cancer: quality of life, economic impact, and survivorship implications, J. Psychosoc. Oncol. 26 (1) (2008) 69–80.
[7] Chinese Anti-Cancer Association, Committee of Lung Cancer Society, Lung Cancer Group of Oncology Branch, Chinese Medical Association, Chinese expert consensus on the multidisciplinary clinical diagnosis and treatment of stage III non-small cell lung cancer, Zhonghua Zhongliu Zazhi 41 (12) (2019) 881–890.
[8] J.L. Wolf, T.E. Trandafir, F. Akram, E.R. Andrinopoulou, A. Maat, D.A.M. Mustafa, J.M. Kros, A.P. Stubbs, A.C. Dingemans, et al., The value of prognostic and predictive parameters in early-stage lung adenocarcinomas: a comparison between biopsies and resections, Lung cancer 176 (2023) 112–120.
[9] Z. Cheng, H. Cui, Y. Wang, J. Yang, C. Lin, X. Shi, Y. Zou, J. Chen, X. Jia, et al., The advance of the third-generation EGFR-TKI in the treatment of non-small cell lung cancer, Oncol. Rep. 51 (1) (2024) 1–13.
[10] R. Sun, Z. Hou, Y. Zhang, B. Jiang, Drug resistance mechanisms and progress in the treatment of EGFR-mutated lung adenocarcinoma, Oncol. Lett. 24 (5) (2022) 408.
[11] Q. Wang, A. Zeng, M. Zhu, L. Song, Dual inhibition of EGFR-VEGF: an effective approach to the treatment of advanced non-small cell lung cancer with EGFR mutation, Int. J. Oncol. 62 (2) (2023) 1–10.
[12] L. Chang, S. Fang, W. Gu, The molecular mechanism of metabolic remodeling in lung cancer, J. Cancer 11 (6) (2020) 1403–1411.
[13] K. Rubio, A.J. Romero-Olmedo, P. Sarvari, G. Swaminathan, V.P. Ranvir, D.G. Rogel-Ayala, J. Cordero, S. Günther, A. Mehta, et al., Non-canonical integrin signaling activates EGFR and RAS-MAPK-ERK signaling in small cell lung cancer, Theranostics 13 (8) (2023) 2384–2407.
[14] E. Castellanos, E. Feld, L. Horn, Driven by mutations: the predictive value of mutation subtype in EGFR-mutated non-small cell lung cancer, J. Thorac. Oncol. 12 (4) (2017) 612–623.
[15] V. Aran, J. Omerovic, Current approaches in NSCLC targeting K-ras and EGFR, Int. J. Mol. Sci. 20 (22) (2019) 5701.
[16] Y. Lei, Y. Lei, X. Shi, J. Wang, EML4-ALK fusion gene in non-small cell lung cancer, Oncol. Lett. 24 (2) (2022) 277.
[17] J. He, Z. Huang, L. Han, Y. Gong, C. Xie, Mechanisms and management of 3rd-generation EGFR-TKI resistance in advanced non-small cell lung cancer, Int. J. Oncol. 59 (5) (2021) 1–20.
[18] J. Wu, Z. Lin, Non-small cell lung cancer targeted therapy: drugs and mechanisms of drug resistance, Int. J. Mol. Sci. 23 (23) (2022) 15056.
[19] W. Meng, J. Meng, F. Zhang, H. Jiang, X. Feng, F. Zhao, K. Wang, Sulforaphane overcomes T790M-mediated gefitinib resistance in vitro through epithelial-mesenchymal transition, J. Physiol. Pharmacol. 72 (5) (2021) 741–749.
[20] Z. Tariq, M. Blyly, A durable response to osimertinib in an elderly patient with EGFR T790M positive metastatic non-small-cell lung cancer after progression on erlotinib, Am. J. Ther. 30 (5) (2023) e463–e465.
[21] N. Yanagitani, K. Uchibori, S. Koike, M. Tsukahara, S. Kitazono, T. Yoshizawa, A. Horiike, F. Ohyanagi, Y. Tambo, et al., Drug resistance mechanisms in Japanese anaplastic lymphoma kinase-positive non-small cell lung cancer and the clinical responses based on the resistant mechanisms, Cancer Sci. 111 (3) (2020) 932–939.
[22] L.A. Byers, L. Diao, J. Wang, P. Saintigny, L. Girard, M. Peyton, L. Shen, Y. Fan, U. Giri, et al., An epithelial-mesenchymal transition gene signature predicts resistance to EGFR and PI3K inhibitors and identifies Axl as a therapeutic target for overcoming EGFR inhibitor resistance, Clin. Cancer Res. 19 (1) (2013) 279–290.
[23] J. Liu, R. Kang, D. Tang, The KRAS-G12C inhibitor: activity and resistance, Cancer Gene Ther. 29 (7) (2022) 875–878.

[24] L.A. Pikor, V.R. Ramnarine, S. Lam, W.L. Lam, Genetic alterations defining NSCLC subtypes and their therapeutic implications, Lung cancer 82 (2) (2013) 179–189.
[25] J. Minguet, K.H. Smith, P. Bramlage, Targeted therapies for treatment of non-small cell lung cancer–Recent advances and future perspectives, Int. J. Cancer 138 (11) (2016) 2549–2561.
[26] Z. Chen, H. Duan, X. Tong, P. Hsu, L. Han, S.L. Morris-Natschke, S. Yang, W. Liu, K.H. Lee, Cytotoxicity, hemolytic toxicity, and mechanism of action of pulsatilla saponin D and its synthetic derivatives, J. Nat. Prod. 81 (3) (2018) 465–474.
[27] C. Tang, C.C. Zhao, H. Yi, Z.J. Geng, X.Y. Wu, Y. Zhang, Y. Liu, G. Fan, Traditional Tibetan medicine in cancer therapy by targeting apoptosis pathways, Front. Pharmacol. 11 (1) (2020) 976.
[28] J. Yang, X. Zhu, P. Yuan, J. Liu, B. Wang, G. Wang, Efficacy of traditional Chinese Medicine combined with chemotherapy in patients with non-small cell lung cancer (NSCLC): a meta-analysis of randomized clinical trials, Support. Care Cancer 28 (8) (2020) 3571–3579.
[29] Z. Li, Z. Feiyue, L. Gaofeng, Traditional Chinese medicine and lung cancer–From theory to practice, Biomed. Pharmacother. 137 (1) (2021) 111381.
[30] K. Sun, L. Wu, S. Wang, W. Deng, Anti-tumor effects of Chinese herbal medicine compounds and their nano-formulations on regulating the immune system microenvironment, Front. Oncol. 12 (1) (2022) 949332.
[31] L. Zhang, K. Wei, J. Xu, D. Yang, C. Zhang, Z. Wang, M. Li, Belamcanda chinensis (L.) DC-An ethnopharmacological, phytochemical and pharmacological review, J. Ethnopharmacol. 186 (1) (2016) 1–13.
[32] The Committee for the Pharmacopoeia of PR China, Belamcanda chinensis, The Phamacopoeia of the People's Republic of China 2015 Edition 101 (1) (2015) 285.
[33] Y.P. Guo, P. Yi, Q.Q. Shi, R.R. Yu, J.H. Wang, C.Y. Li, H.Q. Wu, Cytotoxic compounds from Belamcanda chinensis (L.) DC induced apoptosis in triple-negative breast cancer cells, Molecules 28 (12) (2023) 4715.
[34] Y. Guo, Y.H. Chen, Z.H. Cheng, H.N. Ou-Yang, C. Luo, Z.L. Guo, Tectorigenin inhibits osteosarcoma cell migration through downregulation of matrix metalloproteinases in vitro, Anti Cancer Drugs 27 (6) (2016) 540–546.
[35] C. Morrissey, J. Bektic, B. Spengler, D. Galvin, V. Christoffel, H. Klocker, J.M. Fitzpatrick, R.W. Watson, Phytoestrogens derived from Belamcanda chinensis have an antiproliferative effect on prostate cancer cells in vitro, J. Urol. 172 (6) (2004) 2426–2433.
[36] A. Hasibeder, V. Venkataramani, P. Thelen, H.J. Radzun, S. Schweyer, Phytoestrogens regulate the proliferation and expression of stem cell factors in cell lines of malignant testicular germ cell tumors, Int. J. Oncol. 43 (5) (2013) 1385–1394.
[37] M. Liu, S. Yang, L. Jin, D. Hu, Z. Wu, S. Yang, Chemical constituents of the ethyl acetate extract of Belamcanda chinensis (L.) DC roots and their anti-tumor activities, Molecules 17 (5) (2012) 6156–6169.
[38] X. Shi, Y. Jin, C. Chen, H. Zhang, W. Zou, Q. Zhang, Z. Lu, Q. Chen, Y. Lai, et al., Triptolide inhibits bcr-abl transcription and induces apoptosis in sti571-resistant ChronicMyelogenous leukemia cells harboring T315I mutation, Clin. Cancer Res. 15 (5) (2009) 1686–1697.
[39] G. Yu, Y. Shen, L. Chen, X. Xu, J. Yang, Drug-eluting beads bronchial arterial chemoembolization vs. conventional bronchial arterial chemoembolization in the treatment of advanced non-small cell lung cancer, Front. Med. 10 (1) (2023) 1201468.
[40] W. Jing, M. Li, Y. Zhang, F. Teng, A. Han, L. Kong, H. Zhu, PD-1/PD-L1 blockades in non-small-cell lung cancer therapy, OncoTargets Ther. 9 (1) (2016) 489–502.
[41] R.L. Siegel, K.D. Miller, A. Jemal, Cancer statistics, CA. Cancer J. Clin. 66 (1) (2016) 7–30, 2016.
[42] B.C. Bade, C.S. Dela Cruz, Lung cancer 2020: epidemiology, etiology, and prevention, clin. Chest, Med. 41 (1) (2020) 1–24.
[43] J.E. Gong, J.E. Kim, S.H. Park, S.J. Lee, Y.J. Choi, S.I. Choi, Y.W. Choi, H.S. Lee, J.T. Hong, et al., Anti-tumor effects of an aqueous extract of Ecklonia cava in BALB/cKorl syngeneic mice using colon carcinoma CT26 cells, Oncol, Rep. 49 (6) (2023) 128.
[44] H. Matsumoto, S. Ando, E. Yoshimoto, T. Numano, N. Sultana, K. Fukamachi, M. Iinuma, K. Okuda, K. Kimura, et al., Extracts of Musa basjoo induce growth inhibition and changes in the protein expression of cell cycle control molecules in human colorectal cancer cell lines, Oncol. Lett. 23 (3) (2022) 99.
[45] S.F. Chen, Z.Y. Zhang, J.L. Zhang, Matrine increases the inhibitory effects of afatinib on H1975 cells via the IL-6/JAK1/STAT3 signaling pathway, Mol. Med. Rep. 16 (3) (2017) 2733–2739.
[46] X. Lu, J. Mao, Y. Wang, Y. Huang, M. Gu, Water extract of frankincense and myrrh inhibits liver cancer progression and epithelial-mesenchymal transition through Wnt/β-catenin signaling, Mol. Clin. Oncol. 19 (4) (2023) 77.
[47] J. Shi, H. Lv, C. Tang, Y. Li, J. Huang, H. Zhang, Mangiferin inhibits cell migration and angiogenesis via PI3K/AKT/mTOR signaling in high glucose- and hypoxia-induced RRCECs, Mol. Med. Rep. 23 (6) (2021) 473.
[48] J. Estaquier, F. Vallette, J.L. Vayssiere, B. Mignotte, The mitochondrial pathways of apoptosis, Adv. Exp. Med. Biol. 942 (1) (2012) 157–183.
[49] B. Tummers, D.R. Green, Caspase-8: regulating life and death, Immunol. Rev. 277 (1) (2017) 76–89.
[50] S.J. Jeon, E.Y. Choi, E.J. Han, S.W. Lee, J.M. Moon, S.H. Jung, J.Y. Jung, Piperlongumine induces apoptosis via the MAPK pathway and ERK-mediated autophagy in human melanoma cells, Int. J. Mol. Med. 52 (6) (2023) 115.
[51] J. Zhang, L. Darman, M.S. Hassan, U. Von Holzen, N. Awasthi, Targeting KRAS for the potential treatment of pancreatic ductal adenocarcinoma: recent advancements provide hope, Oncol. Rep. 50 (5) (2023) 1–16.
[52] S.H. Han, J.H. Lee, J.S. Woo, G.H. Jung, S.H. Jung, E.J. Han, Y.S. Park, B.S. Kim, S.K. Kim, et al., Myricetin induces apoptosis through the MAPK pathway and regulates JNK-mediated autophagy in SK-BR-3 cells, Int. J. Mol. Med. 49 (4) (2022) 54.
[53] V. Asati, D.K. Mahapatra, S.K. Bharti, PI3K/Akt/mTOR and Ras/Raf/MEK/ERK signaling pathways inhibitors as anticancer agents: structural and pharmacological perspectives, Eur. J. Med. Chem. 109 (1) (2016) 314–341.
[54] M. Song, N. Zhang, F. Cao, J. Liu, PKNOX2 suppresses lung cancer cell proliferation by inhibiting the PI3K/AKT/mTOR axis, Exp. Ther. Med. 25 (5) (2023) 217.
[55] H. Davies, G.R. Bignell, C. Cox, P. Stephens, S. Edkins, S. Clegg, J. Teague, H. Woffendin, M.J. Garnett, et al., Mutations of the BRAF gene in human cancer, Nature 417 (6892) (2002) 949–954.
[56] Q. Liu, X. Jiang, W. Tu, L. Liu, Y. Huang, Y. Xia, X. Xia, Y. Shi, Comparative efficiency of differential diagnostic methods for the identification of BRAF V600E gene mutation in papillary thyroid cancer, Exp. Ther. Med. 27 (4) (2024) 1–12.
[57] G. Bollag, P. Hirth, J. Tsai, J. Zhang, P.N. Ibrahim, H. Cho, W. Spevak, C. Zhang, Y. Zhang, et al., Clinical efficacy of a RAF inhibitor needs broad target blockade in BRAF-mutant melanoma, Nature 467 (7315) (2010) 596–599.
[58] G.V. Long, D. Stroyakovskiy, H. Gogas, E. Levchenko, F. de Braud, J. Larkin, C. Garbe, T. Jouary, A. Hauschild, et al., Combined BRAF and MEK inhibition versus BRAF inhibition alone in melanoma, N. Engl. J. Med. 371 (20) (2014) 1877–1888.
[59] O.V. Ojulari, J.B. Chae, S.G. Lee, K. Min, T.K. Kwon, J.O. Nam, Apoptotic effect of jaceosidin on MCF-7 human breast cancer cells through modulation of ERK and p38 MAPK pathways, Nat. Prod. Res. 35 (24) (2021) 6049–6053.
[60] L.X. Lv, Z.X. Zhou, Z. Zhou, L.J. Zhang, R. Yan, Z. Zhao, L.Y. Yang, X.Y. Bian, H.Y. Jiang, et al., Hispidin induces autophagic and necrotic death in SGC-7901 gastric cancer cells through lysosomal membrane permeabilization by inhibiting tubulin polymerization, Oncotarget 8 (16) (2017) 26992–27006.
[61] S. Srinual, P. Chanvorachote, V. Pongrakhananon, Suppression of cancer stem-like phenotypes in NCI-H460 lung cancer cells by vanillin through an Akt-dependent pathway, Int. J. Oncol. 50 (4) (2017) 1341–1351.
[62] P. Jantaree, K. Lirdprapamongkol, W. Kaewsri, C. Thongsornkleeb, K. Choowongkomon, K. Atjanasuppat, S. Ruchirawat, J. Svasti, Homodimers of vanillin and apocynin decrease the metastatic potential of human cancer cells by inhibiting the FAK/PI3K/Akt signaling pathway, J. Agric. Food Chem. 65 (11) (2017) 2299–2306.
[63] P. Verma, A. Ghosh, M. Ray, S. Sarkar, Lauric acid modulates cancer-associated microRNA expression and inhibits the growth of the cancer cell, Anti Cancer Agents Med. Chem. 20 (7) (2020) 834–844.
[64] S. Sundarraj, R. Thangam, V. Sreevani, K. Kaveri, P. Gunasekaran, S. Achiraman, S. Kannan, γ-Sitosterol from Acacia nilotica L. induces G2/M cell cycle arrest and apoptosis through c-Myc suppression in MCF-7 and A549 cells, J. Ethnopharmacol. 141 (3) (2012) 803–809.